https://doi.org/10.1016/j.measurement.2015.12.024

Uncertainty estimation of an indexed metrology platform for the verification of portable coordinate measuring instruments.

R. Acero[1*], J. Santolaria[2], M. Pueo[1], J. Abad[3]

1 Centro Universitario de la Defensa. Academia General Militar. Ctra. Huesca s/n. 50090, Zaragoza, Spain
2 Department of Design and Manufacturing Engineering, University of Zaragoza. María de Luna 3, 50018 Zaragoza, Spain
3 Department of Mechanical Engineering, University of Zaragoza. María de Luna 3, 50018 Zaragoza, Spain

* Corresponding author. Tel. +34 976739831, fax +34 976739824, E-mail: racero@unizar.es

KEYWORDS: uncertainty, indexed metrology platform, Monte Carlo

This work presents the development of an uncertainty estimation procedure for an indexed metrology platform. The use of an indexed metrology platform in calibration and verification procedures for portable coordinate measuring instruments, enables the evaluation of different working volumes of the instrument that rotates with the platform in six rotating positions without moving the gauge from a fixed location, reducing in this way the testing time and test setups in comparison with the tests included in the applicable standards. The platform is able to express points in a global reference coordinate system located in the lower platform through its mathematical model. Due to the platform model complexity and according to the GUM supplement 1, the propagation of distributions using the Monte Carlo method was applied to estimate the platform measurement uncertainty. The different error sources affecting the platform uncertainty were first identified. An analysis of the dynamic behavior of the platform by means of a computational and experimental modal test was done in this work. The capacitive sensors assembled in the platform determine the position and orientation of the upper platform with respect to the lower platform and were selected as input variables of the model with their related errors. The n-homogeneous transformation matrices obtained in the simulation as output variables will allow the coordinate reference system change from the upper platform to the lower platform. In this way, it is possible to estimate the influence of the indexed metrology platform position and orientation uncertainty in the generation of points in a global reference system and as a consequence, its influence in a distance measurement.

1. Introduction

According to the GUM supplement 1 [1], the measurement uncertainty estimation through distributions propagation using the Monte Carlo method gives a guidance for measurement uncertainty expression when the conditions for the GUM uncertainty framework [2] are not fulfilled or it is difficult to apply it due to the complexity of the model [3]–[5]. The approach is based on the n-iterations repetition of sampling from the probability distribution function of the input variables and the evaluation of the model in each event. The following stages are carried out in the uncertainty estimation procedure developed in this work:

- Selection of the output variable Y
- Definition of the input variables X_i upon Y depends and their probability distribution functions
- Development of the mathematical model liking the input variables X_i and the output variable Y
- Propagation of the input variables probability distribution functions through the model to obtain the output variable probability distribution function.
- Estimation of the output variable Y most probable value, its uncertainty as a standard deviation and the confidence interval.

Extensive literature in regard to the use of the Monte Carlo method in measurement uncertainty estimation procedures have been identified [3], [6], applied to coordinate measuring machines (CMMs) uncertainty analysis [4], [5], [7]–[9] or to articulated arm coordinate measuring machines (AACMM) as is Romdhani et al. [10] and in Ostrowska [11].

This work focus on the uncertainty estimation of an indexed metrology platform (IMP) using the Monte Carlo method due to the complex mathematical model of the platform. The indexed metrology platform is an auxiliary instrument to be used in calibration and verification procedures for portable coordinate measuring instruments (PCMMs) to evaluate their volumetric accuracy and repeatability [12]. Brau et al. [13] proposed the use of this platform whose main advantage resides in the reduction of the time and physical effort required to carry out these type of procedures. This is achieved by fixing the calibrated gauge object and placing the AACMM on the IMP's upper platform throughout the verification procedure, in comparison with the conventional procedures established in the standards ASME B89.4.22-2004 standard [14], VDI/VDE 2617-2009 part 9 guideline [15] and ISO/CD 10360 part 12 -2014 draft [16]. It is the portable measuring instrument placed on the IMP the one that rotates jointly with the upper platform during the verification procedure, enabling a great coverage of the AACMM's working volume and the definition of a broad number of testing positions but

avoiding the movement of the calibrated gauge object during the verification. Moreover, not only testing and set up times are reduced with the use of the IMP, but also the space needed in the data capturing process is diminished since the number of physical testing positions of the gauge are minimized. Each time the platform rotates to a new position allowing the AACMM to measure the same point in the gauge, the values of the AACMM's encoders change, and therefore a new working volume of the instrument is evaluated. The IMP is composed of two hexagonal platforms, one fixed lower platform and a mobile upper platform which rotates around the fixed one every 60º allowing the definition of six different positions, see Fig. 1. The mechanical repeatability of the platform is achieved by means of kinematic couplings configuration of spheres and cylinders. Three reference spheres located on each platform, allow the determination of the reference systems of both platforms and the possibility to express the coordinates of a captured point by the AACMM in the fixed lower platform global coordinate system during the verification procedure. By means of a mathematical model explained in Brau et al. [13] a homogenous transformation matrix (HTM) is found allowing the change of the coordinate reference systems required. The IMP has also a high mechanical position repeatability, being capable of measuring with high precision the orientation and position of the upper platform with respect to the lower platform. This feature is accomplished with the use of six capacitive sensors with nanometer resolution and measuring range of 100 μm for an output voltage from 10 to -10 V and an operational range from 100 to 200 μm with their sensors and targets assembled in the upper and lower platforms respectively.

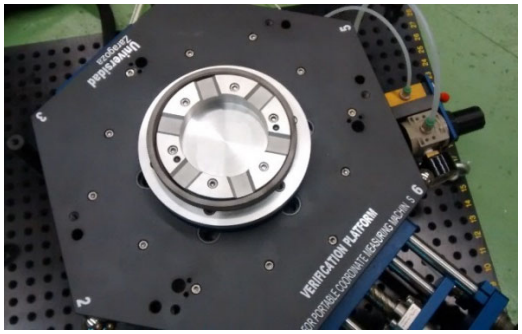

Fig. 1. Indexed metrology platform

2. Model input variables definition

Prior to evaluate the uncertainty of the indexed metrology platform model, it is necessary to define and select the model input variables X_i which could affect the output variable Y. In this case, the possible error sources that may influence the uncertainty of the indexed metrology platform are the platform calibration uncertainty, the capacitive sensors assembled in the platform, the error of the portable measuring equipment that will be used with the platform, the temperature and the dynamic behavior of the platform during the measuring process.

The *calibration procedure* of the indexed metrology platform uses a geometric mathematical model based on the readings and the geometric features of the six capacitive sensors and their corresponding targets. In the calibration process of the platform, the readings of the capacitive sensors will be used as measurement values and the results obtained in the measurement with a coordinate measuring machine (CMM) will be considered as calibrated values, correcting the capacitive sensor ones. The final target of the indexed metrology platform calibration is to determine from the readings of the capacitive sensors a homogeneous transformation matrix that will allow a coordinate reference system change from the upper to the lower platform where the global coordinate reference system is located. The matrix obtained is a single matrix per point measured during the calibration or verification procedure of the portable coordinate measuring instrument. Once all the geometric features of the sensors and the corresponding targets are obtained and expressed in the global coordinate reference system, an identification procedure of the optimum geometric features is launched. These parameters will be the ones that will minimize the difference between the distance measured with the capacitive sensor and the distance calculated through the indexed metrology platform mathematical calibration model. In the platform's uncertainty estimation procedure developed in this work, the calibration uncertainty of the platform has not been included as an input variable but it will be subject of future working lines.

Every *portable coordinate measuring instrument* like articulated arm coordinate measuring machines or a laser trackers, has an error that will influence the results of the measurement. In the case of the articulated arm coordinate measuring machine used in this work, model Faro Platinum, the parameters reported by the manufacturer are a volumetric accuracy of $\pm$ 43 μm and a point repeatability of 30 μm. These parameters will affect the verification procedure using the indexed metrology platform and the generation of the homogeneous transformation matrix to change from the portable measuring instrument coordinate reference system to the upper platform reference system. This matrix is obtained out of the measurement of the three reference spheres located in the upper platform and it is consequently affected by the error of the instrument. Despite this fact, the target of this work was to develop an uncertainty estimation model for the indexed metrology platform without considering the portable measuring instrument, and as a consequence, the uncertainty of the measuring instrument was not included in the Monte Carlo simulation as an input variable.

The analysis of the *dynamic behavior of the platform* and the possible modal deformation of the structure due to the portable instrument's mass, its movement during the measuring process or any external excitation, will be subject of this work and a modal test

is carried out in order to foresee performance of the platform. Also the *temperature* could affect the measurement of the capacitive sensors because of the contraction and expansion of the sensor and target in the measurement procedure, influencing therefore the uncertainty of the indexed metrology platform. Nevertheless the temperature effect has not been included in this first uncertainty estimation of the indexed metrology platform but it will be further developed. The final error source identified that could affect the indexed metrology platform uncertainty are the *capacitive sensors* and the errors that they include in the measuring process, being presented a further detailed analysis in this paper.

2.1. Dynamic performance analysis of the indexed metrology platform and modal test

In order to characterize the dynamic performance of the indexed metrology platform and intending to reproduce its operating conditions, it is carried out in this work a finite element mode analysis of the platform, generating a mathematical model of the structure and a further modal test to predict the vibration properties of the structure in the form of its modal properties – natural frequencies and mode shapes. In this way, it is possible to analyze the influence of external excitement in the measurements made with the capacitive sensors assembled in the indexed metrology platform. The modal test consist on measurements of the vibration behavior of the structure, trying to characterize and explain it. The modal test measures both the response and the excitation defining a relation between both factors [17]. A very important requirement of the modal test is to ensure that all necessary parameters are measured. We carried out a computational modal test with the software Abaqus, generating previously a simplified model of the indexed metrology platform with the finite elements method. Afterwards an experimental modal test of the platform is done in order to validate the natural frequencies and vibration modes obtained in the computational approach.

2.1.1 Computational modal test of the indexed metrology platform

As a first step of the computational modal test, it is necessary to make a finite element meshing of the indexed metrology platform which is based on a simplified model of the structure. The simplified model is similar in properties to the real model, reduces the number of elements and the geometry complexity, minimizing the computational cost derived. The simplification criteria assumed to generate the simplified model were to eliminate elements without specific technical requirements and remove elements whose masses could be considered as insignificant in comparison with the total mass of the platform or not relevant to the rigidity of the structure. The simplified model obtained for the indexed metrology platform versus the real model of the platform could be seen in Fig. 2. Additionally, it is necessary to define the materials of the components in the model and their specific use, information that is summarized in Table 1.

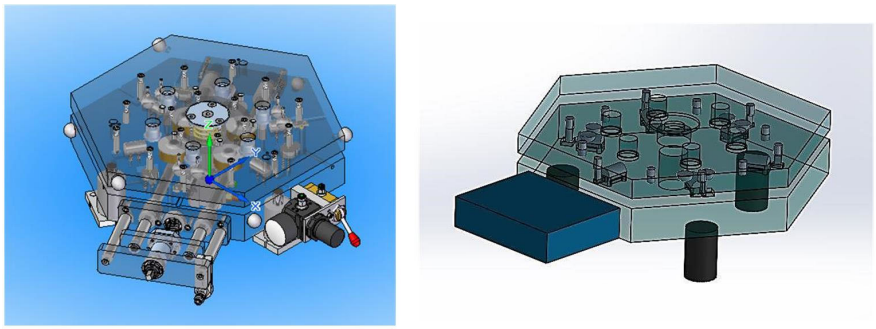

(a) (b)

Fig. 2. Complete CAD model and simplified model of the indexed metrology platform

Table 1. Bill of materials of the indexed metrology platform simplified model.

Component	Material
Kinematic coupling spheres	F131 steel
Kinematic coupling cilinders	F115 steel
Upper and lower platform	F114 steel
Other elements	F111 steel

All these materials are thermal treatment steels and they are selected according to the specific requirements of each platform's component. Their main properties to be taken into account for the frequencies and vibration modes calculation are their density, Young module and Poisson ratio.

- Density = 7800 kg/m^3
- Young module = 210000 MPa
- Poisson ratio = 0.33

Once the simplified model is defined, we proceed with the finite element meshing by means of tetrahedral elements. The mesh generates 260000 elements approximately as it could be observed in Fig. 3 (a) and in Fig. 3 (b) showing a detail of the kinematic couplings cylinder – sphere meshing. Afterwards, the suspension and boundary conditions of the structure must be defined, allowing to reproduce the operating conditions of the model in an accurate and reliable way. Two tests are carried out according to the suspension conditions chosen, the fixed conditions modal test that tries to simulate the real fixing conditions of the structure and the free – free or suspended modal test.

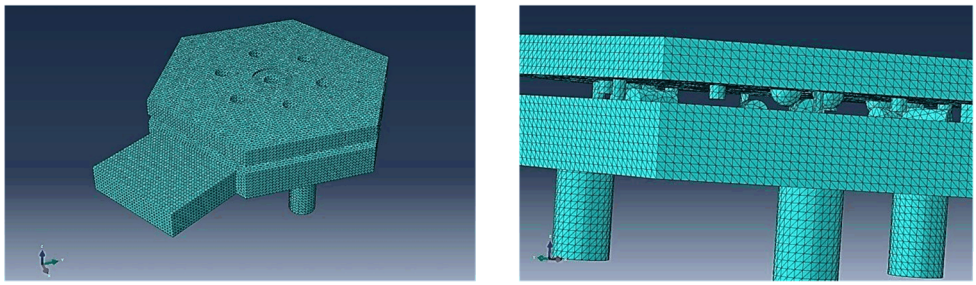

(a) (b)

Fig. 3. Simplified model meshing of the indexed metrology platform.

2.1.1.1 Free-free computational modal test results

This calculation is based on the consideration of an ideal suspended model without interactions with the ambient, obtaining in this way the vibration modes and natural frequencies of the structure. The vibration modes obtained in the free-free modal test are listed in the Table 2. In Fig. 4 the nine first vibration modes are represented.

Table 2. Vibration modes in the free-free computational modal test.

Vibration modes	Rad/s	Frequency (Hz)
1	6.3827e+006	1.0158e+006
2	9.4384e+006	1.5022e+006
3	1.063e+007	1.6918e+006
4	1.0983e+007	1.748e+006
5	1.1248e+007	1.7902e+006
6	1.2043e+007	1.9166e+006
7	1.2398e+007	1.9732e+006
8	1.4485e+007	2.3053e+006
9	1.4826e+007	2.3596e+006

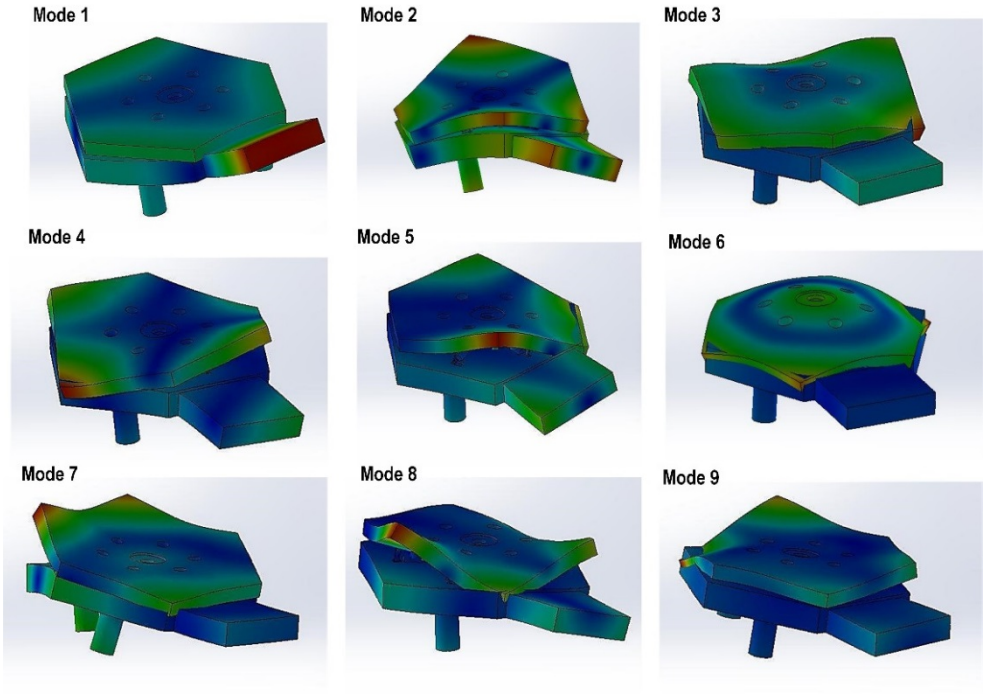

Fig. 4. Vibration modes in the free – free computational modal test

2.1.1.2 Fixed conditions computational modal test results

The indexed metrology platform was designed to be used in a fixed location on a flat and horizontal surface which will be considered as the real fixed conditions. These fixed boundary conditions will not allow any displacement and rotation of the platform with respect to the horizontal surface. The vibration modes obtained in the fixed conditions modal test are included in the Table 3. In Fig. 5 the first nine vibration modes are represented.

Table 3. Vibration modes in the fixed conditions computational modal test.

Vibration mode	Rad/s	Frequency (Hz)
1	9.4304e+006	1.5009e+006
2	1.0531e+007	1.676e+006
3	1.0894e+007	1.7338e+006
4	1.1264e+007	1.7927e+006
5	1.2249e+007	1.9494e+006
6	1.3469e+007	2.1436e+006
7	1.4816e+007	2.3581e+006
8	1.5422e+007	2.4546e+006
9	1.5632e+007	2.4879e+006

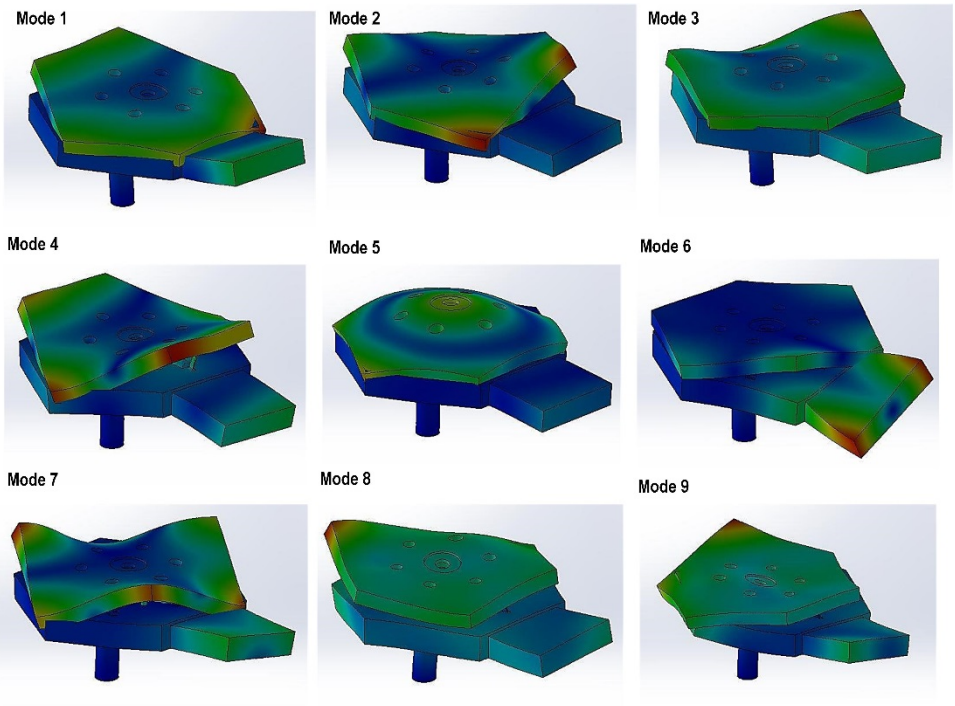

Fig. 5. Vibration modes in the fixed conditions computational modal test

As a conclusion of the results obtained in both computational modal tests, it could be remarked that the indexed metrology platform behaves as an extremely rigid structure due to the high natural frequencies obtained. These frequencies have values between 1000000 Hz and 2500000 Hz with both boundary conditions analyzed, free-free and fixed conditions. In the real operating conditions of the platform, the normal frequencies affecting the indexed metrology platform measurement should not be higher than 1000 Hz, being significantly smaller than the ones obtained in the modal test simulations. Hence, it could be concluded that the modal deformation of the platform will not be significant in the measuring process, with special relevance to the capacitive sensor readings.

2.1.2 Experimental modal test of the indexed metrology platform

An experimental modal analysis is normally structured in three different phases: pre-processing, measurement and post-processing.

a) *Pre-processing*: preparation of the structure for the test, definition of the geometry and the measurement configuration.
The boundary conditions should be defined according to the ones already settled for the computational modal test in order to be able to validate the computational results obtained. In this case and considering the operating conditions of the indexed metrology platform, the platform will be tested under real operating conditions with the platform fixed on a horizontal flat surface on the ground of the laboratory. Once the testing boundary conditions are defined, it is necessary to determine the structure's geometrical model, defining the mesh so that each node will correspond to a response measuring position. In addition, the number of measuring points, excitations points and positions are established, considering the results obtained in the computational modal test. In this case, six excitation points are located on the six corners of the platform where the modal deformation shows its higher values in the computational modal test, see Fig. 4 and Fig. 5. A triaxial accelerometer model Brüel & Kjaer 4506B with a measurement range up to 3000 Hz is positioned in the platform's corner corresponding to the platform position 1. A modal hammer with metallic tip model Endevco 2302-10 is used for the excitation of the structure, being the response captured with the triaxial accelerometer and the signal further treated by the software MTC Hammer under Pulse platform version 9.0. Three measurement repetitions per impact point are made to evaluate the dispersion of the results. The maximum frequency range of the equipment is 25000 Hz, therefore the vibration modes and frequencies registered will be between 0 and 25000 Hz. The impact sequence, excitation and measurement points previously defined and explained for the modal test are shown in Fig. 6.

b) *Measurement*: acquisition of the raw data that will be used to construct the dynamic model of the structure. A controlled excitation force is applied with the hammer and measured together with the resulting responses at the defined points. The measured data will be presented in the form of response functions which are ratio series between responses and excitations. In this case, we will use the frequency response function (FRF) which describes the response to an arbitrary harmonic excitation.

c) *Post-processing:* modal model generation, interpretation and validation. For each model excitation, the structure behavior is captured in the established frecuencial range. The frequency response function (FRF) and coherence function are generated. The coherence function has values between 0 and 1, being unitary its value in the resonance peaks of the structure shown in the FRF function.

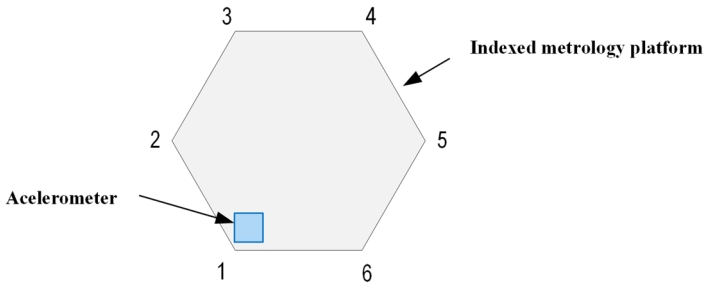

Fig. 6. Excitation sequence definition in the platform experimental modal test

2.1.2.1 Experimental modal test results

Following the test criteria previously explained, the experimental modal test of the platform is carried out obtaining the vibration modes and natural vibration frequencies listed in Table 4. During the test, only three natural vibration frequencies were captured, see Fig. 7 and Fig. 8. The first two modes are identified at frequencies around 1000 Hz and there is a third vibration mode of the platform close to 2000 Hz.

Table 4. Vibration modes and frequencies in the experimental modal test.

Vibration mode	Frequency (Hz)
1	964.5
2	991.9
3	1879

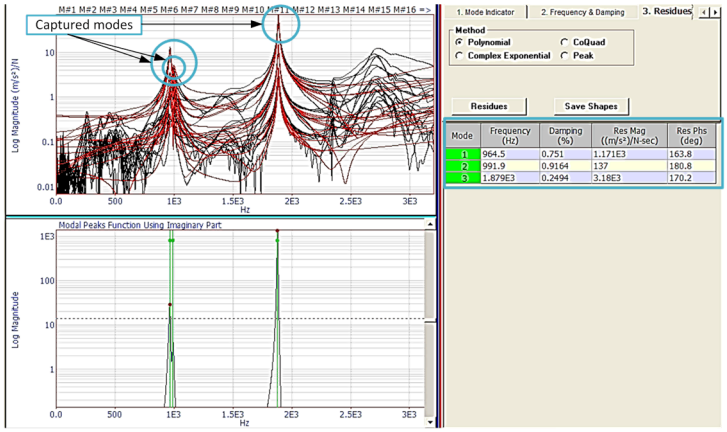

Fig. 7. Frequency response function (FRF) of the indexed metrology platform experimental modal test

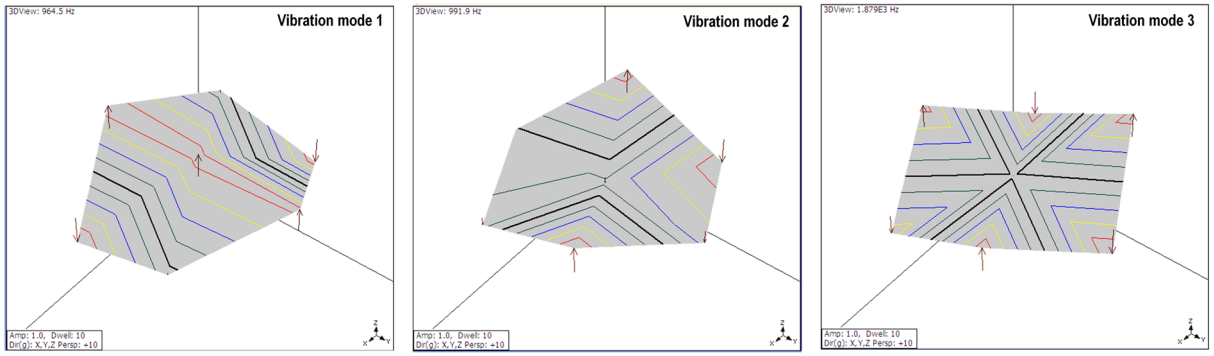

Fig. 8. Vibration modes and frequencies in the platform experimental modal test: mode 1 (964,5 Hz), mode 2 (991,9 Hz) and mode 3 (1879 Hz)

According to the results obtained in the experimental modal test, there are clear discrepancies with the results found in the computational modal test. In the computational one, the vibration modes appeared at higher frequencies over 1000000 Hz. On the

contrary, the experimental modal test shows three vibration modes all of them before the 2000 Hz frecuencial range. There could be further modes over the measuring range of the equipment 25000 Hz, which could not be visible in this analysis. Consequently, two hypothesis are here presented. The first one lays on the fact that the computational modal test perhaps is not reproducing the real operating conditions of the platform, being more rigid that it was expected. Then it would be necessary an adaptation of the model to obtain correlations between the real and the simulated model. It appears in this moment the need to observe if the indexed metrology platform is vibrating during the modal test as a whole, because the vibration frequencies are related to the total mass of the structure. The second hypothesis is based on the consideration that the experimental modal test could be only capturing the vibration modes of the upper platform with lower mass and natural frequencies, being not possible therefore to extrapolate the results to the real model of the platform. In order to reproduce this second hypothesis, a new computational modal test simulating only the upper platform is carried out obtaining frequencies and vibration modes closer to the results of the experimental modal test, as it could be seen in Table 5 and Fig. 9. Two vibration modes are identified at 1170,3 Hz and 1184 Hz, being the third mode found at 2211,9 Hz. These results simulating only the upper platform allow to validate the results obtained in the experimental modal test included in Table 4 and Fig. 8.

Table 5. Vibration modes and frequencies in the upper platform computational modal test

Vibration modes	Frequency (Hz)
1	1170.3
2	1184
3	2211.9

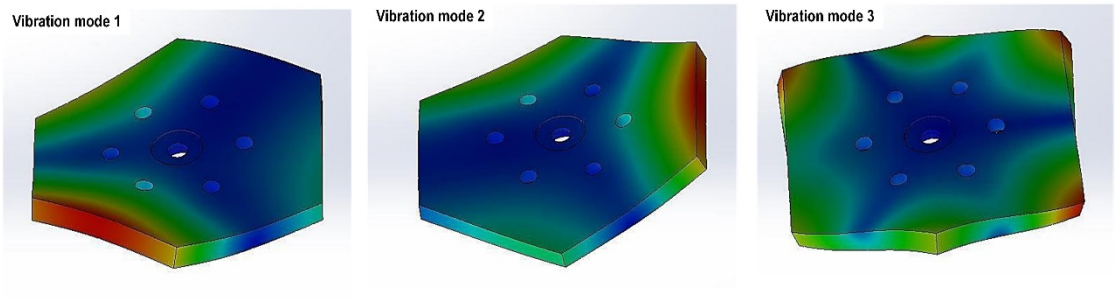

Fig. 9. Vibration modes in the upper platform computational modal test: mode 1 (1170.3 Hz), mode 2 (1184 Hz) and mode 3 (2211.9 Hz)

As a conclusion of the modal tests done in order to evaluate the dynamic performance of the platform, it could be stated that the modal deformation of the platform will not be relevant in the measuring process due to the proved extremely rigid behavior of the structure under external excitations.

2.2. Capacitive Sensor effect in the Monte Carlo simulation

The last error source considered in the analysis are the capacitive sensors assembled in the indexed metrology platform. The values captured with the capacitive sensors will be the inputs X_i of the model. The six capacitive sensors used are model Lion Precision C5-E. The sensors will be affected by some specific errors that could generate variations in the real sensor measurement, being the most relevant ones the sensitivity error, offset error, linearity error and the band error. It is important also to point out the resolution of the sensor. In this analysis, there were taken into account the band error and the sensor resolution. The *band error* accounts for a combination of the linearity and sensitivity errors. It is the measurement of the worst case absolute error in the calibrated range and it is calculated by comparing the output voltages at specific gaps to their expected value. The worst case error from this comparison is listed as the system's error band and is given by the manufacturer as a percentage of the measurement of the sensor. Assuming a normal probability distribution and given a sensor measuring range of 100 µm, it is possible to simulate the band error of the sensor.

The capacitive sensor resolution indicates the smallest realiable measurement possible and it is a measurement of the noise voltage of the probe being bandwith dependent. In the manufacturer calibration report, two resolution values are listed - the peak to peak resolution and the RMS resolution. The peak to peak resolution is measured as the maximum peak to peak output voltage occurring over a period of time, long enough to include low frequency components with the probe fixed. The RMS resolution is the standard deviation of the output voltages sampled over a period of time, long enough to include low frequency components with the probe fixed on a stationary target. The value of RMS resolution was the one taken into account to affect the readings of the capacitive sensors.

Once the main errors affecting the capacitive sensors are described, it is necessary to point out that the band error and RMS resolution values included in the calibration report of the manufacturer will the ones affecting the simulated input readings of the capacitive sensors in the Monte Carlo simulation. The calibration parameters considered by the manufacturer are listed in Table 6 and the errors reported in the calibration procedure of the capacitive sensors are included in Table 7.

Table 6. Capacitive sensors calibration parameters (*source: Lion Precision*)

Calibration parameters	
Output	10 a -10 VDC
Near gap	100 µm
Range	100 µm
Sensitivity	0.2 V/µm
Band width	6000 Hz

Table 7. Capacitive sensors calibration results. Temperature: 24.2ºC. Humidity: 35.5% RH *(source: Lion Precision).*

Sensor ID	Peak to peak resolution (nm)	RMS resolution (nm)	Band error (%)	Linearity error (%)
1	59.28	6.85	0.13	0.07
2	76.95	8.90	0.15	0.08
3	76.06	8.79	0.13	0.13
4	55.48	6.41	0.08	0.08
5	75.09	8.68	0.10	0.10
6	82.31	9.52	0.16	0.11

The sensors output noise was experimentally characterized by means of continuous captures for each of the six capacitive sensors in the six rotating positions of the platform under different test conditions that are following explained. A preload force generated with a pneumatic system was used to avoid the upper platform from tipping due to the mass of the AACMM.

- Test 1: Indexed metrology platform with a pneumatic preload force of 4 bar
- Test 2: Indexed metrology platform with AACMM assembled in static condition with a pneumatic preload force of 4 bar
- Test 3: Indexed metrology platform with AACMM assembled in dynamic condition with a pneumatic preload force of 4 bar

The first test registered the continuous captures of the sensors only applying the preload, without being the measuring instrument assembled on the platform. The test 2 focuses on analyzing the effect of the AACMM's mass on the platform and the measurement with the capacitive sensors, meanwhile the test 3 checks how the AACMM's mass and its movement during the measurement affects the measuring results. It was defined a fixed movement sequence of the AACMM measuring three points on a virtual gauge located in the working volume of the AACMM. During the 20 seconds test duration, 1000 captures per second were measured obtaining 20000 readings per sensor and platform position (1-6). The data registered for each sensor were adjusted to a normal probability distribution function obtaining the mean and standard deviation parameters represented in Fig. 10, according to the data registered for each sensor (1-6) in the test 1 and platform position 1. The mean and standard deviation values obtained are listed in Table 8.

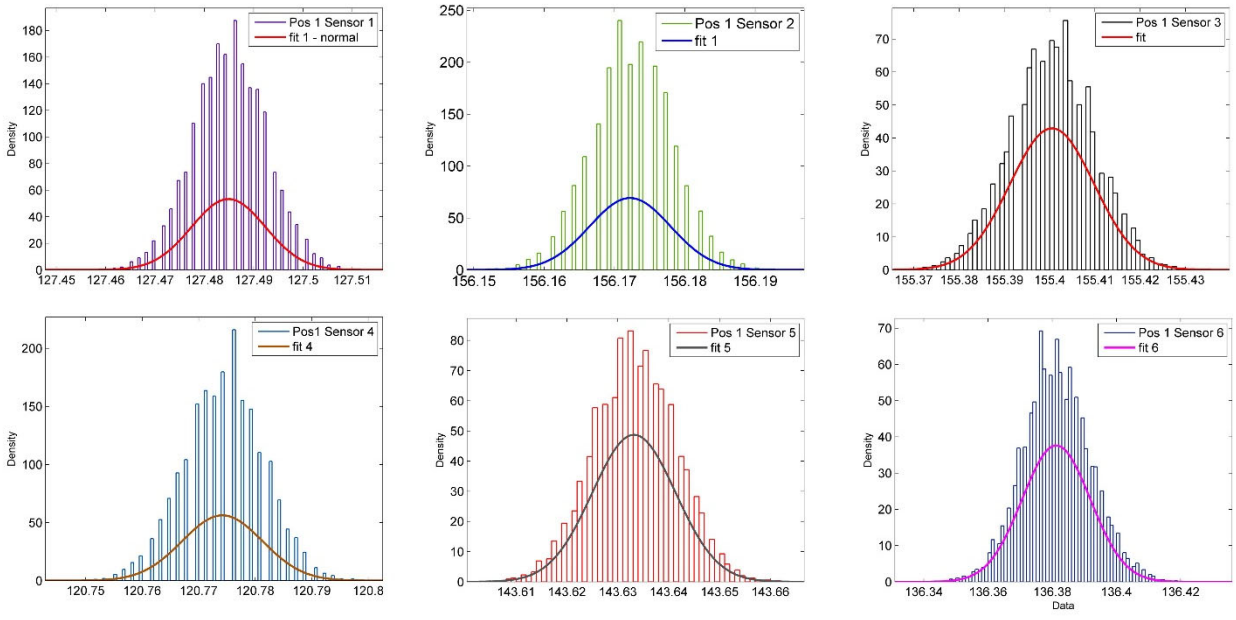

Fig. 10. Normal probability distribution function capacitive sensors (1-6) readings in test 1, platform position 1.

Table 8. Normal probability distribution parameters for capacitive sensors continuous readings, test 1, platform position 1.

Sensor ID	Mean (µm)	Standard deviation (µm)
1	127.4849	0.0075
2	156.1722	0.0058
3	155.4005	0.0093
4	120.7742	0.0071
5	143.6332	0.0082
6	136.3812	0.0106

Comparing the standard deviation values obtained for each sensor with the normal probability distribution adjustment according to the experimental continuous test and the RMS resolution values listed in the sensors' calibration report provided by the manufacturer shown in Table 7, it could be concluded that both data sets are comparable, being the values in the same range as it could be observed in Fig. 11.

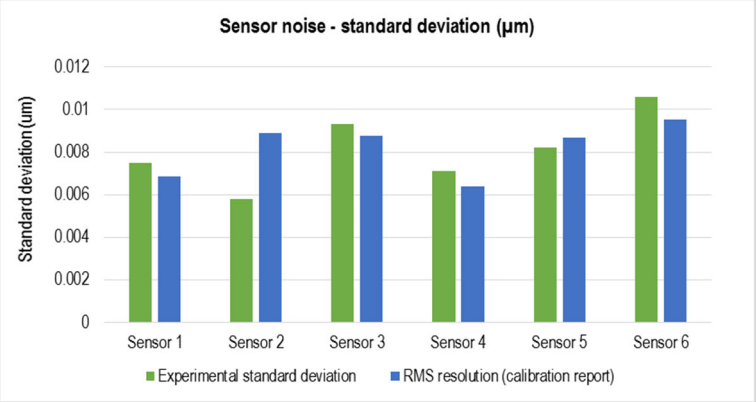

Fig. 11. Sensor noise comparison between calibration report and experimental continuous test 1, platform position 1.

The nominal values of the capacitive sensors to be considered as inputs for the Monte Carlo simulation that will be affected by the sensor noise and the band error given in the calibration report, correspond to the values registered during the measurement of a point on a ball bar gauge sphere with an AACMM assembled on the indexed metrology platform considering a fixed platform and ball bar gauge position. In this work, the experimental measurement was carried out for a ball bar gauge position with radial disposition to the articulated arm coordinate measuring machine represented in Fig. 12. Three platform positions (1/3/6) and three spheres (1/2/5) were evaluated, measuring five points per sphere and capturing simultaneously the readings of the capacitive sensors. As an example, it could be seen in Table 9 the values obtained with each capacitive sensor during the measurement of the first point of the sphere 1 in the platform position 1 for the ball bar gauge position defined.

Table 9. Capacitive sensors nominal readings

Sensor ID	Nominal sensor reading (µm)
1	108.5137
2	125.4271
3	144.3024
4	118.7031
5	148.8462
6	109.1777

The simulated readings of the six capacitive sensors affected by the band error and noise values that will be the inputs for the Monte Carlo simulation model for 100000 iterations are shown in Fig. 13.

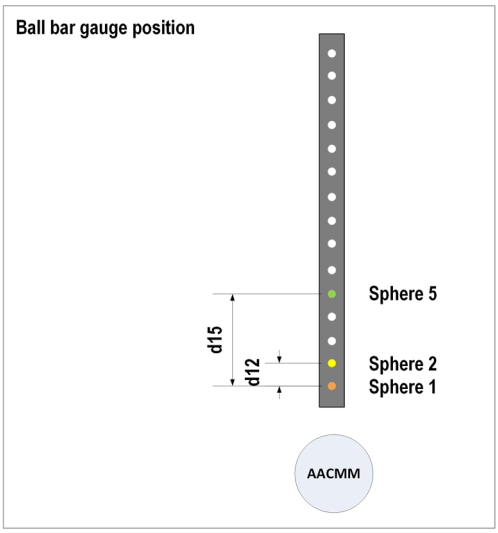

Fig. 12. Ball bar gauge position

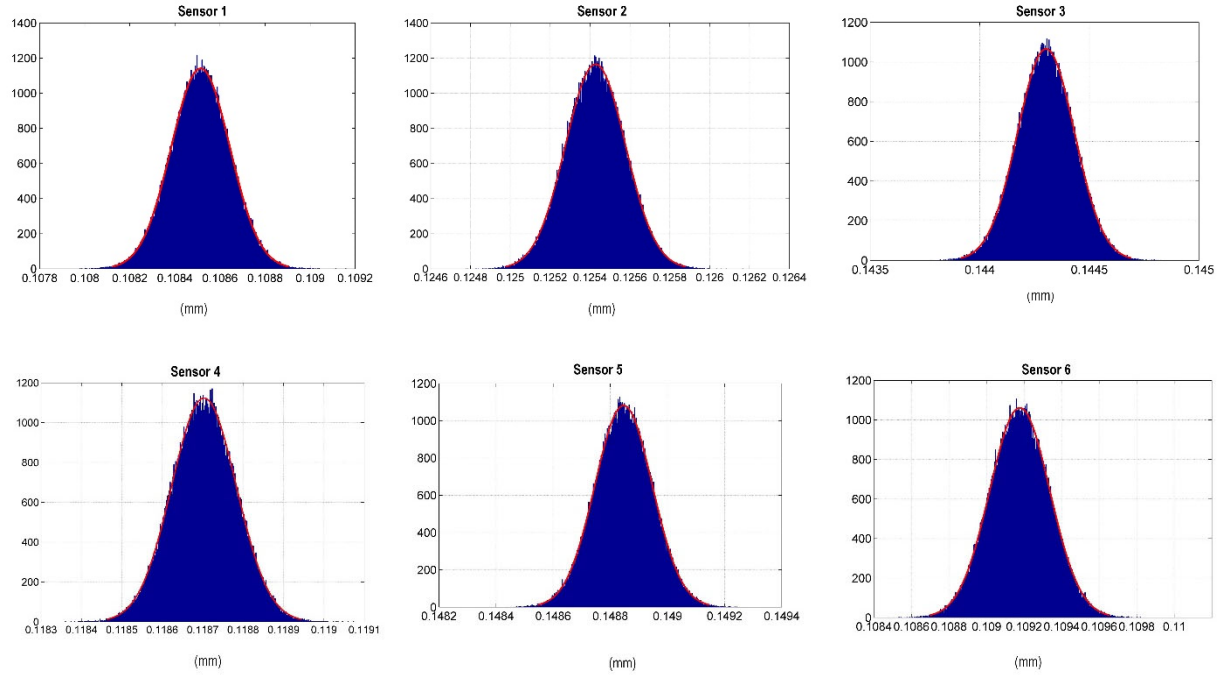

Fig. 13. Capacitive sensors (1-6) simulated readings from platform position 1, sphere 1, point 1, n-iterations 100000

3. Model output variable definition

The output variable Y of the model will be in this case the homogeneous transformation matrix that allow the change from the upper platform coordinate reference system RS $_{UpperPlatform}$ to the lower platform or global coordinate reference system RS $_{LowerPlatform}$ by means of the mathematical model of the indexed metrology platform [13]. This mathematical model generates a single homogeneous transformation matrix per point measured with the measuring instrument assembled on the platform, and will make it possible to express a point captured by the instrument in the global coordinate reference system, based on the capacitive sensor readings per point measured and the geometric optimized parameters obtained in the calibration of the platform. The homogeneous transformation matrix will have translational terms (XYZ) and rotational terms (ABC) which will be considered as the output parameters of the model.

- X→ Translation along the X axis
- Y→ Translation along the Y axis
- Z→ Translation along the Z axis
- A→ Rotation around the X axis
- B→ Rotation around the Y axis
- C→ Rotation around the Z axis

Considering the n-iterations to be carried out in the Monte Carlo simulation, the output will be a matrix with dimension nx6 being n the numbers of iterations, see equation (1).

$$\begin{pmatrix} x_i & \cdots & C_i \\ \vdots & \ddots & \vdots \\ x_n & \cdots & C_n \end{pmatrix} \tag{1}$$

The n-values obtained for each output parameter corresponding to the homogeneous transformation matrix terms could be adjusted to a probability distribution function calculating for each parameter a mean value, an uncertainty value and the confidence interval, being the input values of the model the simulated readings (L1-L6) for the six capacitive sensors previously explained, as could be seen in Fig. 14.

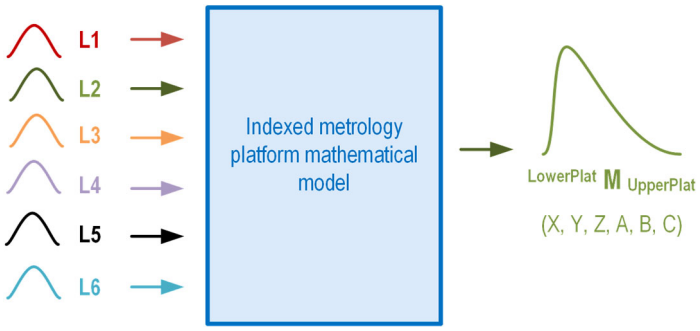

Fig. 14. Input variables probability distribution propagation through the indexed metrology platform model and output variable.

With the n-homogeneous transformation matrices obtained in the simulation that allow the coordinate reference system change from the upper platform to the lower platform, and given a point measured with the AACMM on a ball bar gauge sphere from a platform position with coordinates (x,y,z) expressed in the AACMM coordinate reference system RS_{AACMM}, it is possible to obtain n-points (x,y,z) expressed in the lower platform reference system $RS_{LowerPlat}$ or global reference system RS_{Global}.

In this way, we could estimate the influence of the position and orientation uncertainty of the indexed metrology platform in the generation of points in a global reference system. Additionally and taking into account the m-points measured per sphere expressed in the AACMM coordinate reference system RS_{AACMM}, we could generate from the n-points obtained for each of the m-points measured per sphere and expressed in the global coordinate reference system RS_{Global}, the centers of the corresponding n-Gaussian spheres and the distances between their centers, being able to estimate as a result the influence of the indexed metrology platform's uncertainty in the measurement of a distance. All these concepts are graphically represented in Fig. 15 showing the uncertainty model of the indexed metrology platform.

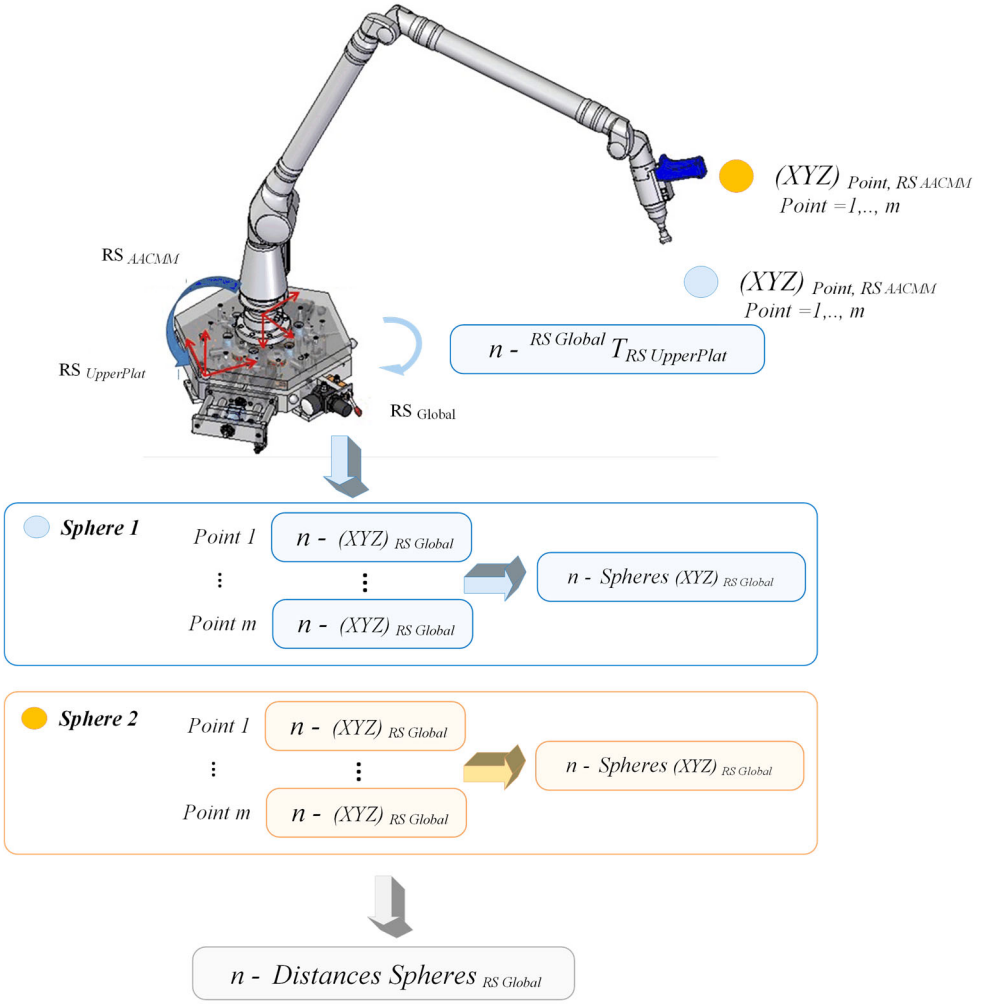

Fig. 15. Indexed metrology platform uncertainty estimation model

4. Uncertainty estimation results

The results obtained out of the simulation for n-iterations, show as output variable the n-homogeneous transformation matrices that allow the coordinate reference system change from the upper platform to the lower platform through the mathematical model of the indexed metrology platform. On these grounds, it is feasible to estimate the indexed metrology platform's position and orientation uncertainty for a given platform position and point measured with the measuring instrument, AACMM in this case. The uncertainty values calculated in this work are expanded uncertainty values.

Taking as a reference the capacitive sensor readings corresponding to the point 1 of the sphere 1 in the ball bar gauge position represented in Fig. 12 from the platform position 1 and 10000 iterations, the translational (XYZ) and rotational (ABC) terms of the 10000 homogeneous transformation matrices are obtained as output parameters of the simulation. The mean, maximum, minimum, upper and lower bound of the 95% confidence interval together with the uncertainty as a standard deviation value, are then calculated and listed in Table 10.

Table 10. Indexed metrology platform position and orientation expanded uncertainty XYZ (μm) - ABC (º) in homogeneous transformation matrices upper to lower platform, sphere 1, point 1, n-iterations 10000

${}^{RS\ Global}T_{RS\ UpperPlat}$ ***(Sphere 1 / Point 1 / Platform position 1)***							
	Nominal	**Mean**	**Uncertainty**	**Maximum**	**Minimum**	**U. bound** (95%)	**L. bound** (95%)
X (mm)	-0.13500	-0.13502	0.01996	-0.13494	-0.13510	-0.13498	-0.13506
Y (mm)	196.61710	196.61707	0.04489	196.61724	196.61691	196.61716	196.61698
Z (mm)	40.84180	40.84181	0.04965	40.84200	40.84159	40.84190	40.84171
A (º)	179.99880	179.99879	0.02057	179.99888	179.99871	179.99883	179.99875
B (º)	0.01940	0.01941	0.01677	0.01948	0.01935	0.01944	0.01938
C (º)	60.05620	60.05621	0.01159	60.05625	60.05616	60.05623	60.05618

Given a point measured on a sphere for fixed positions of the ball bar gauge and the platform, it is possible to analyze the effect of the indexed metrology platform's uncertainty in the generation of the homogeneous transformation matrix through the mathematical model of the platform. Fig. 16 shows all the possible values obtained in the Monte Carlo simulation for the translational XYZ and rotational terms ABC of the 10000 matrices obtained. In addition Fig. 17 shows the uncertainty ellipsoids for the translational terms XYZ and their corresponding projections.

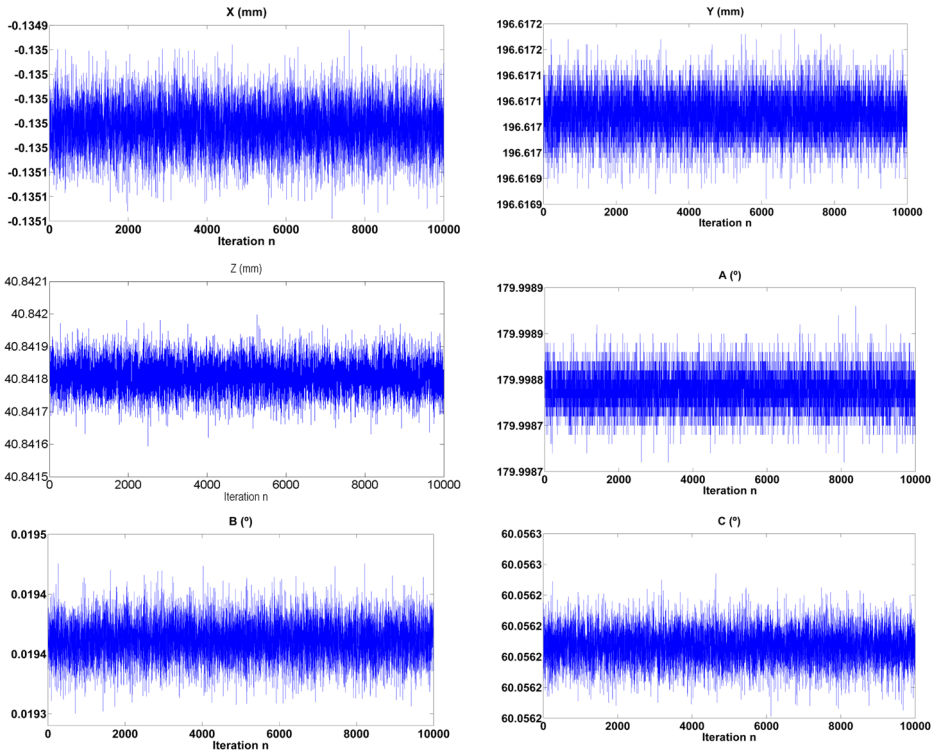

Fig. 16. Simulated homogeneous transformation matrix translational XYZ and rotational ABC terms, n-iterations 10000.

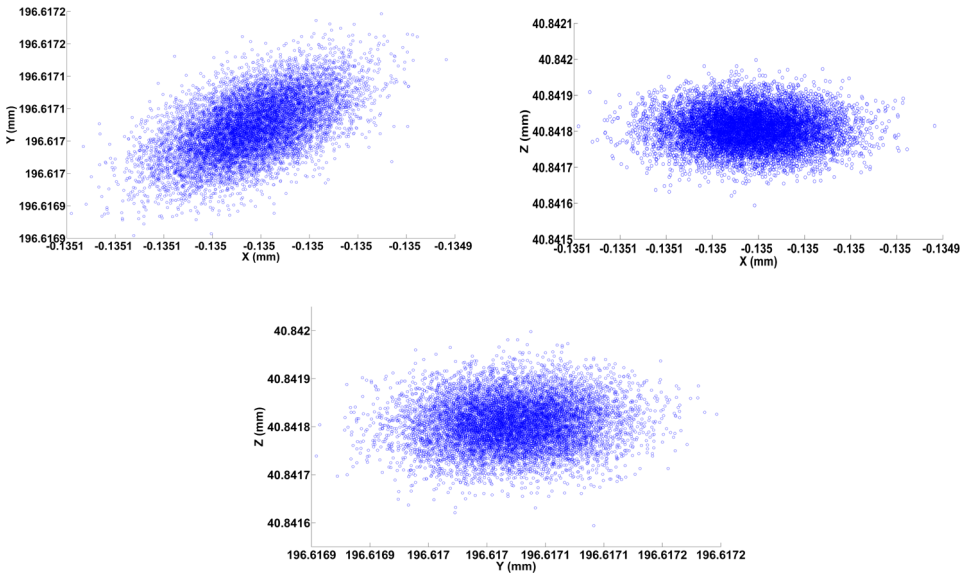

Fig. 17. Uncertainty ellipsoids for the homogeneous transformation matrix translational terms XYZ, n-iterations 10000.

4.1. Evaluation of the indexed metrology platform uncertainty in the generation of a point expressed in the global coordinate reference system.

Once the n-homogeneous transformation matrices to change from the upper to the lower platform reference systems are obtained in the Monte Carlo simulation, it is possible to generate n-points with their coordinates (x,y,z) expressed in the lower platform or global reference system, given a point measured in a gauge sphere with the arm for specific positions of the gauge and the indexed metrology platform. Hence, the influence of the uncertainty of the indexed metrology platform in the generation of points in the global coordinate reference system could be assessed, as it is shown in the uncertainty model explained in Fig. 15. With the n – homogeneous

transformation matrices with values listed in Table 10 and given a point measured in the sphere 1 with coordinates (x,y,z) expressed in RS_{AACMM}, we could simulate n-points in the global platform reference system RS_{Global} corresponding to the point measured in the sphere 1. Running 10000 iterations and considering five points measured in the sphere 1 of the ball bar gauge and the indexed metrology platform in the position 1, the results obtained in the simulation are the following:

Table 11. Indexed metrology platform expanded uncertainty in the generation of the point 1 of the sphere 1 in RS_{Global}, n-iterations 10000.

Point 1 – Sphere 1 (Platform position 1)							
	Nominal	**Mean**	**Uncertainty** (μm)	**Maximum**	**Minimum**	**L. bound** (95%)	**U. bound** (95%)
X (mm)	-57.34600	-57.34600	0.23224	-57.34517	-57.34703	-57.34645	-57.34554
Y (mm)	687.25450	687.25450	0.26270	687.25552	687.25333	687.25398	687.25501
Z (mm)	744.99564	744.99564	0.19425	744.99640	744.99492	744.99526	744.99602

Table 12. Indexed metrology platform expanded uncertainty in the generation of the point 2 of the sphere 1 in RS_{Global}, n-iterations 10000.

Point 2 – Sphere 1 (Platform position 1)							
	Nominal	**Mean**	**Uncertainty** (μm)	**Maximum**	**Minimum**	**L. bound** (95%)	**U. bound** (95%)
X (mm)	-62.03535	-62.03535	0.23086	-62.03438	-62.03627	-62.03580	-62.03489
Y (mm)	699.27579	699.27579	0.25906	699.27678	699.27469	699.27528	699.27629
Z (mm)	733.34541	733.34541	0.19850	733.34622	733.34475	733.34502	733.34580

Table 13. Indexed metrology platform expanded uncertainty in the generation of the point 3 of the sphere 1 in RS_{Global}, n-iterations 10000.

Point 3 – Sphere 1 (Platform position 1)							
	Nominal	**Mean**	**Uncertainty** (μm)	**Maximum**	**Minimum**	**L. bound** (95%)	**U. bound** (95%)
X (mm)	-68.32018	-68.32018	0.22942	-68.31929	-68.32109	-68.32063	-68.31973
Y (mm)	684.46708	684.46707	0.25985	684.46807	684.46609	684.46657	684.46758
Z (mm)	736.63710	736.63711	0.19406	736.63784	736.63625	736.63673	736.63749

Table 14. Indexed metrology platform expanded uncertainty in the generation of the point 4 of the sphere 1 in RS_{Global}, n-iterations 10000.

Point 4 – Sphere 1 (Platform position 1)							
	Nominal	**Mean**	**Uncertainty** (μm)	**Maximum**	**Minimum**	**L. bound** (95%)	**U. bound** (95%)
X (mm)	-53.63718	-53.63718	0.22671	-53.63630	-53.63801	-53.63762	-53.63674
Y (mm)	676.14141	676.14141	0.25829	676.14248	676.14051	676.14090	676.14192
Z (mm)	735.19406	735.19406	0.19052	735.19476	735.19328	735.19369	735.19443

Table 15. Indexed metrology platform expanded uncertainty in the generation of the point 5 of the sphere 1 in RS_{Global}, n-iterations 10000.

Point 5 – Sphere 1 (Platform position 1)							
	Nominal	**Mean**	**Uncertainty** (μm)	**Maximum**	**Minimum**	**L. bound** (95%)	**U. bound** (95%)
X (mm)	-45.98916	-45.98916	0.23146	-45.98831	-45.99008	-45.98961	-45.98870
Y (mm)	693.07839	693.07855	0.26153	693.07959	693.07743	693.07803	693.07906
Z (mm)	735.16236	735.16224	0.19956	735.16299	735.16153	735.16185	735.16263

Fig. 18 (a) shows the tridimensional ellipsoid for the 10000 possible values for the point 1 of the sphere 1 obtained in the Monte Carlo simulation and Fig. 18 (b) represents the 10000 possible values for the coordinates (x,y,z) of the same point 1 of the sphere 1.

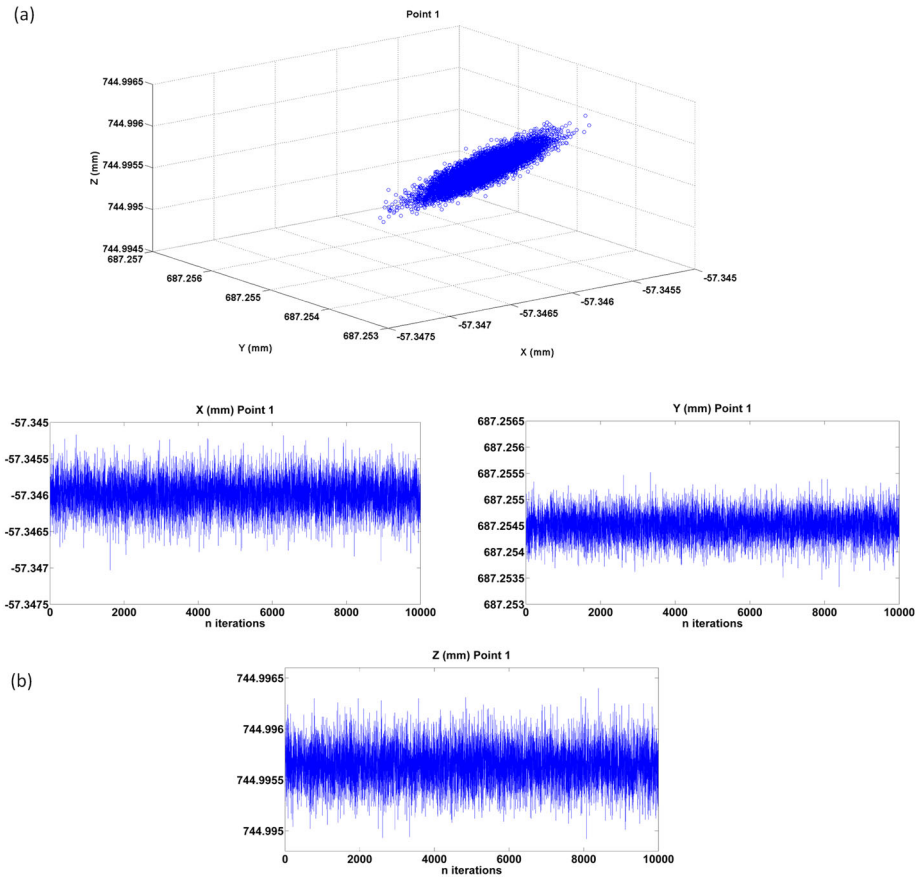

Fig. 18. Possible values of the point 1 – sphere 1 coordinates XYZ expressed in the global coordinate reference system, n-iterations 10000.

In addition and taking into account the five points measured on each sphere being expressed their coordinates in the arm's reference coordinate system, it is possible to generate out of the 10000 points obtained in the simulation for each of the five points measured per sphere, the centers of the 10000 Gaussian spheres expressed in the global coordinate reference system as shown in Fig. 19.

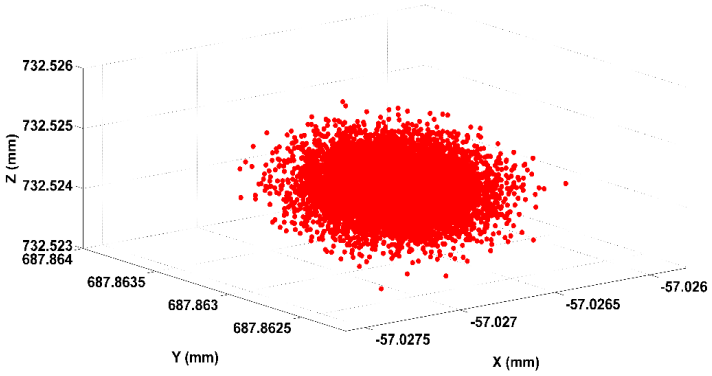

Fig. 19. Possible values of the center coordinates XYZ of the n-spheres 1 expressed in the global coordinate reference system, n-iterations 10000.

4.2. Evaluation of the indexed metrology platform uncertainty in the measurement of different positions of the sphere gauge

The same Monte Carlo simulation procedure done for the sphere 1 was replicated for the spheres 2 and 5 of the ball bar gauge measuring five points on each sphere. In this way, n-homogeneous transformation matrices to change from the upper to the lower coordinate reference system and the n- corresponding points with coordinates expressed in the global reference system, were obtained for each of the five points measured on each sphere.

We analyzed in the simulation the variation of the uncertainty of the platform, depending on the sphere measured according to their position in the ball bar gauge shown in Fig. 12, for the same ball bar position and platform position 1. This variation could be due to several reasons, being one of them the change of the arm angular encoder's readings depending on the distance and the position of the

sphere with respect to the arm. In this work, the simulation was done for 10000 iterations for the spheres 1, 2 and 5 with the uncertainty comparative results listed in Table 16 and Fig. 20 for the coordinates (x,y,z) of the 10000 points obtained in the global platform reference system for the five points measured on each sphere.

Table 16. Comparison of indexed metrology platform expanded uncertainties per sphere measured (1, 2, 5), n-iterations 10000.

		Uncertainty (µm)		
		Sphere 1	**Sphere 2**	**Sphere 5**
Point 1	X (mm)	0.232241	0.241225	0.269990
	Y (mm)	0.262705	0.265127	0.266787
	Z (mm)	0.194251	0.225467	0.315529
Point 2	X (mm)	0.230860	0.239216	0.270039
	Y (mm)	0.259056	0.263258	0.266019
	Z (mm)	0.198503	0.230363	0.319403
Point 3	X (mm)	0.229417	0.241851	0.272184
	Y (mm)	0.259851	0.265617	0.268567
	Z (mm)	0.194056	0.225515	0.315342
Point 4	X (mm)	0.226707	0.238836	0.267329
	Y (mm)	0.258289	0.262216	0.268738
	Z (mm)	0.190516	0.221844	0.316312
Point 5	X (mm)	0.231457	0.241063	0.271587
	Y (mm)	0.261532	0.263736	0.266704
	Z (mm)	0.199563	0.228499	0.319692
Sphere diameter		0.33016	0.34805	0.33449

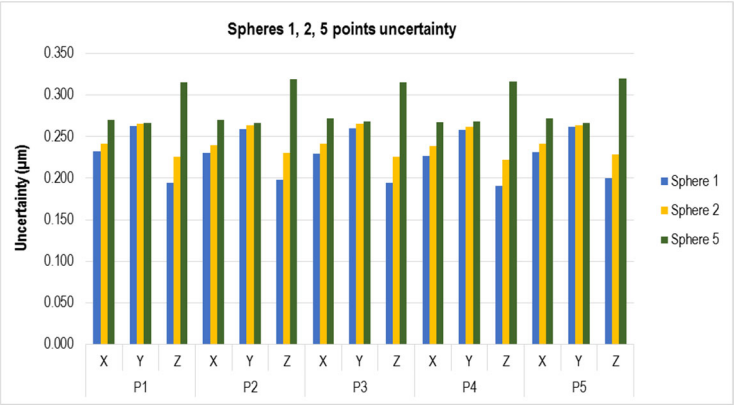

Fig. 20. Indexed metrology platform expanded uncertainty in the measurement of different positions of the sphere gauge, n-iterations 10000.

In the former Table 16 and Fig. 20 it could be observed that the uncertainty has lower values for all the coordinates and points measured in the case of the sphere 1, being the sphere 5 the one with the highest uncertainty values. This fact could be due to the position of the spheres in the ball bar gauge with respect to the arm, see Fig. 12. The sphere 5 is located in the furthest position and therefore the variations in the orientation of the platform's reference system due to the uncertainty of the platform could affect more. The 10000 possible values of the sphere 2 and sphere 5 centers expressed in the global reference system RS_{Global} could be seen in Fig. 21.

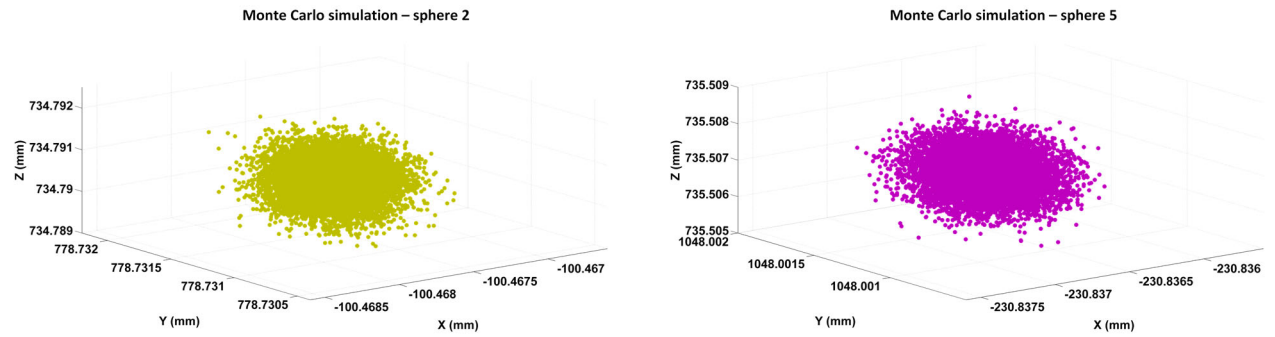

Fig. 21. Possible values of the center coordinates XYZ of the n-spheres 2 and 5 expressed in the global coordinate reference system, n-iterations 10000.

4.3. Evaluation of the indexed metrology platform uncertainty in a distance measurement

The concept is based on the evaluation of a distance error as the deviation between the euclidean distance calculated between the centers of two spheres in the ball bar gauge and the calibrated distance. The target is to analyze by means of the Monte Carlo simulation how the uncertainty of the indexed metrology platform affects the measurement of a distance with the measuring instrument, articulated arm coordinate measuring machine in this case. The distance deviation is calculated according to the equation (2), being L_i the length between centers of the measured spheres and L_{Cal} the calibrated length.

$$D_i = L_i - L_{Cal} \tag{2}$$

After obtaining the 10000 simulated centers for each of the spheres 1, 2 and 5, it is possible to calculate the distance between their centers for the 10000 spheres generated, observing how the uncertainty of the indexed metrology platform affects in the measurement of these distances. Thus two nominal calibrated distances are established, the distance between the centers of the spheres 1 and 2 named as d12 and a longer distance d15 between the centers of the spheres 1 and 5. The nominal distance values obtained from the calibrated sphere centers included in the calibration report of the ball bar gauge are listed in Table 17.

Table 17. Calibrated lengths definition in the ball bar gauge

	d12 (Sphere 1 - 2)	**d15 (Sphere 1 - 5)**
Calibrated length (mm)	100.80247	399.96137

As a final result of this evaluation, five parameters are calculated: the mean, maximum and minimum distance error, the standard deviation and the range of distance deviations with the results included in the Table 18. These parameters were used to evaluate the influence of the indexed metrology platform's uncertainty in a distance measurement with the measuring instrument.

Table 18. Indexed metrology platform expanded uncertainty and error parameters in a distance measurement, n-iterations 10000

	d12 (Sphere 1 - 2)	**d15 (Sphere 1 - 5)**
Mean distance error (mm)	0.058721	0.063400
Maximum distance error (mm)	0.059636	0.064404
Minimum distance error (mm)	0.057635	0.062562
Distance error range (mm)	0.002001	0.001842
Standard deviation (mm)	0.000245	0.000242

It was observed that the mean distance error is bigger in the case of the longer distance d15 with a value of 0.0634 mm versus the value obtained in the shorter distance d12, 0.0587 mm. The range is slightly lower 0.0018 mm in the longer distance evaluation, with a value of 0.0020 mm for the d12 distance. The standard deviation values obtained are similar for both distances.

4.4. Evaluation of the indexed metrology platform uncertainty influence in the measurement from different platform positions

Finally and in order to analyze the influence of the different rotating positions of the platform in its uncertainty estimation procedure, simulations for the platform positions 3 and 6 were carried out under the same premises considered in the case of the platform position 1 previously explained. The sphere 1 was taken as a reference, measuring five points per sphere and running 10000 iterations in the

simulation. In the following Table 19, it is shown a comparative summary of the uncertainties obtained for the XYZ coordinates of each of the 10000 points generated for the five points measured in the sphere 1 with the AACMM measuring from the platform positions 1, 3 and 6. In addition, it is also included the uncertainty obtained in the spheres diameter calculation for the three positions of the platform evaluated.

Table 19. Comparison of indexed metrology platform expanded uncertainties in the sphere 1 measurement from different platform positions (1, 3, 6), n-iterations 10000.

		Uncertainty (µm)		
Platform position		**1**	**3**	**6**
Point 1	X (mm)	0.237251	0.336581	0.321769
	Y (mm)	0.275764	0.191801	0.189172
	Z (mm)	0.201466	0.208158	0.171014
Point 2	X (mm)	0.220530	0.336820	0.314770
	Y (mm)	0.262204	0.192493	0.185209
	Z (mm)	0.199191	0.212803	0.172280
Point 3	X (mm)	0.238617	0.330789	0.309839
	Y (mm)	0.272784	0.192055	0.189935
	Z (mm)	0.200863	0.210502	0.173191
Point 4	X (mm)	0.232483	0.332145	0.313143
	Y (mm)	0.270231	0.187238	0.188535
	Z (mm)	0.200888	0.203918	0.167066
Point 5	X (mm)	0.227324	0.333095	0.316487
	Y (mm)	0.265404	0.189137	0.188833
	Z (mm)	0.204541	0.207487	0.170702
Sphere diameter		0.342780	0.347125	0.343805

It could be observed in Table 19 and Fig. 22 several platform's behaviors depending of the point coordinate analyzed. For all the five points per sphere, the uncertainty is higher in the X coordinate for the platform position 3. In the case of the Y coordinate, the uncertainty values are always higher for the platform position 1 and for the Z coordinates, the uncertainty is slightly higher for the platform position 3. Neither the five points simulated show bigger uncertainty values for a specific platform position in the three coordinates XYZ, nor any of the platform positions have higher uncertainty values than the others in a representative way. As a conclusion no error trend per platform position could be inferred.

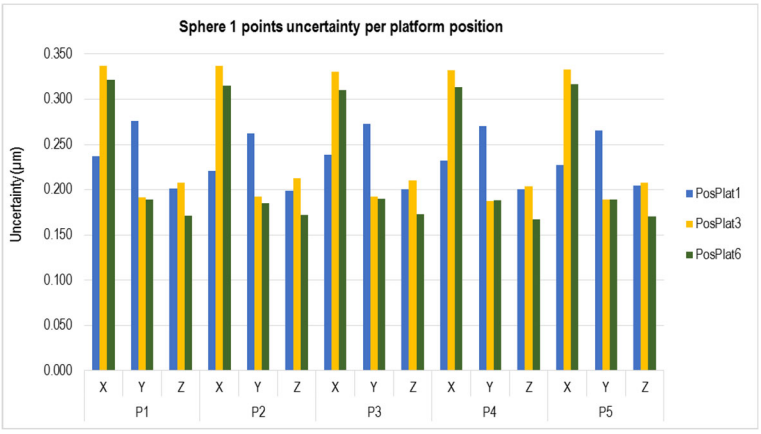

Fig. 22. Indexed metrology platform expanded uncertainty per platform position (1, 3, 6), n-iterations 10000.

In regard to the influence of the number of iterations in the indexed metrology platform's uncertainty calculation with the Monte Carlo method, we run simulations for 10, 100, 1000 and 10000 iterations, fixing finally the trials in 10000 because the variation in the mean value of the output variables was very small between 1000 and 10000 iterations. As an example, the evolution of the X coordinate mean value (mm) for the point 1 measured on the sphere 1 from the platform position 1, during several Monte Carlo simulations with 10, 100, 1000 and 10000 iterations is represented in Fig. 23. The nominal value measured with the AACMM from the platform position 1 of the X coordinate of the point of the sphere 1 mentioned is -57.3459 mm. It is important to point out that the variation in the mean values of the output variable is small, as it is the variation in the readings of the capacitive sensors which are the input variables of the model.

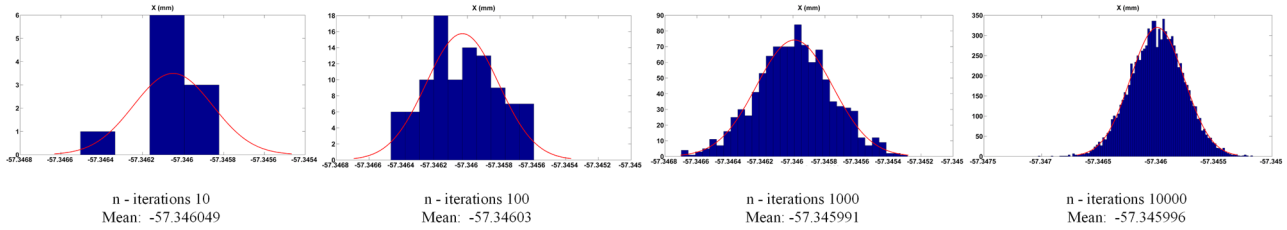

Fig. 23. Iteration number influence in simulation of output parameter X coordinate (mm) of point 1, sphere 1.

5. Conclusions

The indexed metrology platform, as an auxiliary instrument to be used in calibration and verification procedures for portable coordinate measuring instruments, should not influence the measurement results of these procedures. For this reason, it is important to estimate its measurement uncertainty in order to be able to validate the use of the platform in these procedures. This work has developed an uncertainty estimation procedure for the indexed metrology platform based on the Monte Carlo method simulation, identifying as a first step the main error sources that could affect measurement results of the platform. The main error sources found were the calibration uncertainty of the platform, the error of the portable measuring instrument, the capacitive sensors' errors, the possible modal deformation of the platform and the temperature.

In order to characterize the dynamic performance of the indexed metrology platform, it was carried out in this work a finite element mode analysis of the platform, generating a mathematical model of the structure and a further modal test to predict the vibration properties of the structure in the form of its modal properties. The computational modal test showed that the platform behaved as an extremely rigid solid with vibration frequencies in the range from 1000000 Hz to 2500000 Hz independently of the boundary conditions settled. The experimental modal test carried out in the laboratory with three excitation sequences trying to reproduce the results obtained in the computational modal test, captured only three vibration modes. The first two modes were found in frequencies close to 1000 Hz and a third one in frequencies around 2000 Hz, not validating the results that were obtained in the computational modal test. The reason was that the vibration modes corresponded only to the upper platform with lower mass, fact that could be proved repeating the computational modal test only for the upper platform with three vibration modes reached in this case between 1100 and 2200 Hz, analogues to the ones in the experimental modal test. As the whole platform behaved as a rigid solid according to the results obtained in the computational modal test, it was decided to remove this error source in the uncertainty calculation of the platform.

Then the platform expanded uncertainty estimation through the Monte Carlo simulation was carried out. First, it was decided to analyze the influence of the capacitive sensors assembled in the platform as input variables of the model, including the band errors and the sensor noise values given by the manufacturer in the calibration report. Given a point measured with the AACMM, the readings of the six capacitive sensors and n-iterations, the output variables of the model will be in this case the n-homogeneous transformation matrices that allow the change from the upper platform coordinate reference system to the lower platform coordinate reference system and the n-points expressed in the lower platform coordinate reference system, being able to estimate in this way the influence of the position and orientation uncertainty of the indexed metrology platform in the generation of points in a global reference system. Additionally and taking into account the m-points measured per sphere expressed in the AACMM coordinate reference system, we could generate from the n-points obtained for each of the m-points measured per sphere and expressed in the global coordinate reference system, the centers of the corresponding n-Gaussian spheres and the distances between their centers, estimating then the influence of the uncertainty of the indexed metrology platform in the measurement of a distance.

Taking as a reference the platform position 1, a fixed ball bar gauge position and the first point measured, the uncertainty obtained for the sphere 1 in the X coordinate was 0.23224 µm, 0.26270 µm in the Y coordinate and 0.19425 mm in the Z coordinate. For the sphere 2, the uncertainty values were 0.24122 µm for the X coordinate, 0.26512 µm for the Y coordinate and 0.22546 µm in Z. Finally in the sphere 5, the values were 0.26999 µm, 0.26678 µm and 0.31552 µm for the X, Y and Z coordinates. It could be concluded that despite the uncertainties are in the same range for all the spheres measured, there are differences in the calculated values depending on the influence of the platform uncertainty because of the variations in the platform's reference coordinate system.

Additionally, there were analyzed the platform uncertainties depending on the position of the platform selected, running the Monte Carlo simulation for the platform positions 1, 3 and 6. For all the points measured in the sphere 1, the uncertainty is bigger in the X coordinate for the platform position 3. In the case of the Y coordinate, the values obtained are always higher for the platform position 1 and the uncertainty is slightly higher in the Z coordinate for the platform position 3. Neither the five points simulated showed bigger uncertainty values for a specific platform's position in the three coordinates XYZ, nor do any of the platform's positions have higher uncertainty values than the others in a representative way. Therefore no error trend per position of the platform could be concluded. The uncertainty of the indexed metrology platform in a distance measurement was also evaluated, with mean error and uncertainty values of 0.058721 ± 0.000245 mm for short distances (100 mm) and 0.063400 ± 0.000242 mm for distances defined as long ones (400 mm). Finally, it is important to point out that an increase in the number of iterations in the Monte Carlo simulation, makes the mean value of the output simulated parameters go closer to the nominal parameter value. In this case, the maximum number of iterations was

10000, because the difference between the mean output parameter values obtained for 1000 and 10000 trials, showed variations of 0.01 μm, value which could be considered small enough to decide not to increase the number of iterations.

6. Bibliography

[1] Joint Committee for Guides in Metrology (JCGM), "JCGM 101 : 2008 Evaluation of measurement data — Supplement 1 to the ' Guide to the expression of uncertainty in measurement ' — Propagation of distributions using a Monte Carlo method." 2008.

[2] International Organization for Standardization – ISO, Ed., *Guide to the expression of uncertainty in measurements, GUM*. Geneva (Switzerland), 2008.

[3] H. Schwenke, B. R. L. Siebert, F. Wäldele, and H. Kunzmann, "Assessment of Uncertainties in Dimensional Metrology by Monte Carlo Simulation: Proposal of a Modular and Visual Software," *CIRP Ann. - Manuf. Technol.*, vol. 49, no. 1, pp. 395–398, 2000.

[4] a. Balsamo, M. Di Ciommo, R. Mugno, B. I. Rebaglia, E. Ricci, and R. Grella, "Evaluation of CMM Uncertainty Through Monte Carlo Simulations," *CIRP Ann. - Manuf. Technol.*, vol. 48, no. 1, pp. 425–428, 1999.

[5] J. M. Baldwin, K. D. Summerhays, D. a. Campbell, and R. P. Henke, "Application of Simulation Software to Coordinate Measurement Uncertainty Evaluation," *Measure*, vol. 2, no. 4, pp. 40–52, 2007.

[6] M. G. Cox and B. R. L. Siebert, "The use of a Monte Carlo method for evaluating uncertainty and expanded uncertainty," *Metrologia*, vol. 43, no. 4. pp. S178–S188, 2006.

[7] J. Sladek and A. Gaska, "Evaluation of coordinate measurement uncertainty with use of virtual machine model based on Monte Carlo method," *Measurement*, vol. 45, no. 6, pp. 1564–1575, Jul. 2012.

[8] J. Beaman and E. Morse, "Experimental evaluation of software estimates of task specific measurement uncertainty for CMMs," *Precis. Eng.*, vol. 34, no. 1, pp. 28–33, 2010.

[9] J. P. Kruth, N. Van Gestel, P. Bleys, and F. Welkenhuyzen, "Uncertainty determination for CMMs by Monte Carlo simulation integrating feature form deviations," *CIRP Ann. - Manuf. Technol.*, vol. 58, no. 1, pp. 463–466, 2009.

[10] F. Romdhani, F. Hennebelle, M. Ge, P. Juillion, R. Coquet, and J. F. Fontaine, "Methodology for the assessment of measuring uncertainties of articulated arm coordinate measuring machines," *Meas. Sci. Technol.*, vol. 25, no. 12, p. 125008, 2014.

[11] K. Ostrowska, A. Gąska, and J. Sładek, "Determining the uncertainty of measurement with the use of a Virtual Coordinate Measuring Arm," *Int. J. Adv. Manuf. Technol.*, vol. 71, no. 1–4, pp. 529–537, Dec. 2013.

[12] R. Acero, A. Brau, J. Santolaria, and M. Pueo, "Verification of an articulated arm coordinate measuring machine using a laser tracker as reference equipment and an indexed metrology platform," *Measurement*, vol. 69, pp. 52–63, 2015.

[13] A. Brau Avila, J. Santolaria Mazo, and J. J. Aguilar Martín, "Design and mechanical evaluation of a capacitive sensor-based indexed platform for verification of portable coordinate measuring instruments.," *Sensors (Basel).*, vol. 14, no. 1, pp. 606–33, Jan. 2014.

[14] American Society of Mechanical Engineers, "ASME B89.4.22-2004, Methods for performance evaluation of articulated arm coordinate measuring machines." New York, NY, USA, pp. 1–45, 2004.

[15] Verein Deutscher Ingenieure, "VDI/VDE 2617 Part 9, Acceptance and reverification test for articulated arm coordinate measuring machines." pp. 1–20, 2009.

[16] International Organization for Standardization, "ISO / CD 10360-12 Geometrical Product Specifications (GPS) — Acceptance and reverification tests for coordinate measuring systems (CMS) — Part 12 : articulated arm coordinate measurement machines (CMM)," Geneva (Switzerland), 2014.

[17] D. J. Ewins, "Basics and state-of-the-art of modal testing," *Sadhana*, vol. 25, no. 3. pp. 207–220, 2000.